

Determination of the linear mass power spectrum from the mass function of galaxy clusters

Ariel G. Sánchez¹, Nelson D. Padilla^{1,2} and Diego G. Lambas^{1,3,4}

¹ *Grupo de Investigaciones en Astronomía Teórica y Experimental, (IATE), Observatorio Astronómico Córdoba, UNC, Argentina.*

² *Dept Physics, University of Durham, South Road, Durham, DH1 3LE.*

³ *Consejo Nacional de Investigaciones Científicas y Tecnológicas (CONICET), Argentina.*

⁴ *John Simon Guggenheim Fellow.*

Accepted 2002 July 23. Received 2002 July 19; in original form 2002 June 25

ABSTRACT

We develop a new method to determine the linear mass power spectrum using the mass function of galaxy clusters. We obtain the rms mass fluctuation $\sigma(M)$ using the expression for the mass function in the Press & Schechter (1974), Sheth, Mo & Tormen (2001) & Jenkins et al. (2001) formalisms. We apply different techniques to recover the adimensional power spectrum $\Delta^2(k)$ from $\sigma(M)$ namely the k_{eff} approximation, the singular value decomposition and the linear regularization method. The application of these techniques to the τ CDM and Λ CDM GIF simulations shows a high efficiency in recovering the theoretical power spectrum over a wide range of scales. We compare our results with those derived from the power spectrum of the spatial distribution of the same sample of clusters in the simulations obtained by application of the classical Feldman, Kaiser & Peacock (1994), FKP, method. We find that the mass function based method presented here can provide a very accurate estimate of the linear power spectrum, particularly for low values of k . This estimate is comparable, or even better behaved, than the FKP solution.

The principal advantage of our method is that it allows the determination of the linear mass power spectrum using the joint information of objects of a wide range of masses without dealing with specific assumptions on the bias relative to the underlying mass distribution.

Key words: Cosmology: Theory – Large Scale Structure of the Universe

1 INTRODUCTION

Cosmological models predict the large scale matter distribution evolved from primordial fluctuations in the density of the universe. Unfortunately this distribution is not directly accessible through observations because we can only observe the distributions of objects like galaxies or clusters of galaxies that do not, necessarily, trace the mass distribution in a simple way.

The power spectrum of the galaxy distribution has proven to be the most popular statistic used to characterize the matter distribution in the universe. This is due to its tight relation to physical properties of the growth of structures throughout the history of the Universe. Also, the many ways and different kind of data that can be used to measure the power spectrum has allowed independent results from redshift and angular galaxy surveys, cluster surveys, and CMB fluctuations studies. Each of these approaches have different drawbacks, though. For instance, the results from large redshift surveys, are subject to several problems since

the results obtained are affected by the incompleteness of the survey, its geometry, the redshift space distortions and the bias factor (which can be scale dependent). Moreover the distribution of galaxies or clusters of galaxies is affected by non-linear evolution effects, which makes it even more difficult to carry out a direct comparison between observational results and theoretical model predictions.

An alternative technique was presented by Gaztañaga & Baugh (1998), and has been applied in different ways by several other authors (Dodelson & Gaztañaga, 2001, Eisenstein & Zaldarriaga, 2001 and references therein). In it the power spectrum of the galaxy distribution is derived from the angular correlation function inverting Limber's equation. As this procedure does not involve any Fourier transforms nor the use of redshift data, the results obtained in this way are not affected by a convolution with the survey window function, nor by redshift space distortions. The principal uncertainty in this approach comes from the fact that one of the ingredients of the technique is the redshift distribu-

tion of galaxies, which may not be accurately known, and moreover the results are still affected by the bias factor and non-linear evolution.

The aim of this work is to develop a new method for obtaining the power spectrum, free of the problems of the methods previously described. In order to do this, we use the formalisms of Press & Schechter (1974, hereafter PS) and Sheth, Mo & Tormen (2001, hereafter SMT) where halos form in the higher peaks of the evolving primordial density fluctuations which are related to the linear power spectrum. This indicates that studying the distribution of halo masses, one can obtain information about the mass distribution, and therefore, recover the mass power spectrum. More precisely, PS's like recipes are sets of equations that allow the determination of the mass function of dark matter halos from the mass power spectrum. If the mass function can be determined observationally, we can use these equations in the inverse way to derive the linear power spectrum.

In this paper we present a new method for determining the linear power spectrum from the mass function of clusters of galaxies based on the PS, SMT and Jenkins et al. (2001, hereafter J01) prescriptions for the mass function of systems expected in hierarchical clustering scenarios.

The outline of the paper is as follows, in section §2 we briefly review the different formalisms for obtaining a mass function used in this work. In §3 we give the general outline of our method and a simple test in an idealized case. In §4 we describe a test of our method by its application to the GIF simulations (Kauffman et al., 1999). In §4 we show a comparison with the results obtained using the standard technique of Feldman, Kaiser & Peacock (1994, hereafter FKP) for measuring the power spectrum, and finally, in §5 we present a short discussion and the main conclusions.

2 THE MASS FUNCTION

An important tool with which to characterize the density field is the rms density fluctuation, smoothed on some co-moving scale R . For the case of a top-hat window, this scale is related to a mass $M = \frac{4\pi}{3}\bar{\rho}R^3$, where $\bar{\rho}$ is the mean density of the universe ($\bar{\rho} = \rho_c\Omega$). In turn, this quantity and the power spectrum $P(k) = |\delta_k|^2$ are related by

$$\sigma(R) = \int_{-\infty}^{\infty} \Delta^2(k) W^2(kR) \, d \ln k \quad (1)$$

where $\Delta^2(k) = \frac{k^3}{2\pi^2} P(k)$ is the dimensionless power spectrum and $W(kR)$ is the Fourier transform of the top-hat window function

$$W(kR) = \frac{3}{kR} j_1(kR) = 3 \frac{(\sin(kR) - kR \cos(kR))}{(kR)^3},$$

where $j_1(x)$ is the spherical Bessel function of order 1.

PS developed a simple formalism to obtain an analytical expression for the differential mass function of dark matter halos based on the spherical collapse model. In this model, the abundance of haloes with masses $M \rightarrow M + dM$ is given by:

$$n(M)dM = \left(\frac{2}{\pi}\right)^{\frac{1}{2}} \frac{\bar{\rho}}{M^2} \frac{\delta_c}{\sigma(M)} \left| \frac{d \ln(\sigma(M))}{d \ln(M)} \right| \quad (2)$$

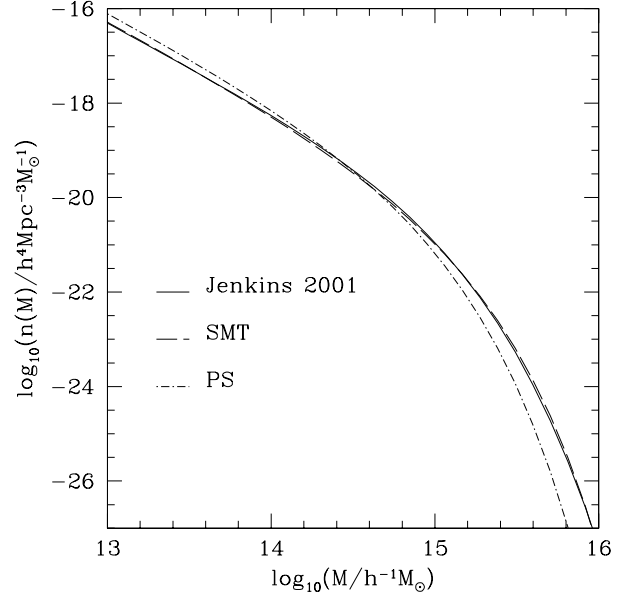


Figure 1. The mass functions predicted by different formalisms for a τ CDM model. The curve obtained from the SMT formalism gives a much better description of the results from numerical simulations (shown by the J01 general fit) than the PS recipe.

$$\times \exp \left[-\frac{\delta_c^2}{2\sigma(M)^2} \right] dM,$$

where δ_c is the density threshold corresponding to collapse according to the spherical collapse model. For an $\Omega = 1$ universe $\delta_c = 1.686$ and its value has little dependence on cosmology (Eke et al., 1996). This function is plotted in Figure 1 for a τ CDM model.

The vague analytical justification in the derivation of expression (2) has lead to different criticisms of the PS formalism (e.g. Peacock & Heavens, 1989), but a later and more formal derivation due to Bond et al. (1991) based on a particular type of filtering, and the set excursion theory, yields the same expression for the mass function according to the spherical collapse model, placing the PS formalism on a more solid theoretical basis. In addition to the original tests presented in PS, equation (2) has been checked against results from a variety of numerical simulations (Efstathiou et al., 1988, Colberg & Couchman, 1989) showing a good general agreement.

Nevertheless, recent works (Tormen, 1998; Sheth & Tormen, 1999, Governato et al. 1999, J01) detected discrepancies between the PS predictions and the halo abundances obtained in much better numerical simulations. The PS formula underestimates the abundances of massive halos and overestimates the low mass end of the mass function (already seen in the earlier numerical simulations results). A better description of the numerical results is given by a correction to the PS mass function proposed originally by Sheth & Tormen (1999)

$$n(M)dM = \sqrt{\frac{2aA^2}{\pi}} \frac{\bar{\rho}}{M^2} \frac{\delta_c}{\sigma(M)} \left[1 + \left(\frac{\sigma(M)}{\sqrt{a}\delta_c} \right)^{2p} \right] \quad (3)$$

$$\times \left| \frac{d \ln(\sigma)}{d \ln(M)} \right| e^{-\left(\frac{a\delta_c^2}{2\sigma^2(M)}\right)} dM \quad (4)$$

where $A = 0.322$, $a = 0.707$ and $p = 0.3$. This function is also plotted in Figure 1. SMT showed that this correction can be understood as a result of the incorporation of the ellipsoidal rather than spherical collapse model dynamics in a formalism similar to the one used by Bond et al. (1991).

We can define a function

$$f(\sigma, z) = \frac{M}{\bar{\rho}} \frac{dn_{cum}(M, z)}{d \ln \sigma^{-1}}, \quad (5)$$

where $n_{cum}(M, z)$ is the cumulative mass function. From (2) and (3) we can calculate $f(\sigma, z)$ for PS and SMT formalisms where

$$f(\sigma; PS) = \sqrt{\frac{2}{\pi}} \frac{\delta_c}{\sigma} \exp\left(-\frac{\delta_c^2}{2\sigma^2}\right) \quad (6)$$

$$f(\sigma; SMT) = \sqrt{\frac{2a}{\pi}} \left[1 + \left(\frac{\sigma^2}{a\delta_c^2}\right)^p\right] \frac{\delta_c}{\sigma} \exp\left(-\frac{a\delta_c^2}{2\sigma^2}\right) \quad (7)$$

That is, the PS and SMT formalisms predict that the function $f(\sigma, z)$ is independent of redshift and the cosmological model when it is expressed in terms of σ .

From the analysis of a set of simulations carried out by the Virgo Consortium, J01 found that the function $f(\sigma)$ can be described with an accuracy better than 20% for different redshifts and initial conditions by the general fit

$$f(\sigma) = A \exp\left(-|\ln \sigma^{-1} + B|^\varepsilon\right), \quad (8)$$

where $A = 0.315$, $B = 0.61$ and $\varepsilon = 3.8$, for halos identified with the FOF algorithm using the same linking length $b = 0.2$ for every value of Ω .

The expression for $n(M)$ inferred from (5) and (8)

$$n(M, z) dM = \frac{A\bar{\rho}(z)}{M^2} \frac{d \ln(\sigma^{-1})}{d \ln(M)} e^{-(|\ln(\sigma^{-1} + B)|^\varepsilon)} dM \quad (9)$$

This differential mass function is also shown in Figure 1, where it can be seen that SMT formalism is in a much better agreement with the general fit of J01 (that is, the results of numerical simulations), than PS formalism.

3 THE METHOD

In this section we analyse the problem of recovering the power spectrum $\Delta^2(k)$ using equation (1) and the expressions for the mass function in the formalisms just described. The steps to be followed in obtaining the linear mass power spectrum are:

(i) Obtain the variance $\sigma(M)$ from the mass function. In order to do this we need to rewrite the expressions relating these statistics.

(ii) Invert the power spectrum from the variance. This involves the application and test of different inversion algorithms.

3.1 Obtaining $\sigma(M)$ from $n(M)$

Assuming the mass function of dark matter haloes obeys one of the three formalisms described in the last section, we can

re-interpret equations (2), (3) and (9) as differential equations and use them in the determination of $\sigma(M)$ provided $n(M)$ is known. In the Appendix we describe the solution of the equations obtained for each formalism.

In the case of PS formalism the final solution is

$$\sigma(M) = \frac{\delta_c}{\sqrt{2} \operatorname{erf}^{-1} \left[\operatorname{erf}\left(\frac{\delta_c}{\sqrt{2}\sigma_8}\right) - \frac{G(M)}{\bar{\rho}} \right]}}, \quad (10)$$

where $\operatorname{erf}(x)$ is the error function and $G(M)$ is given by

$$G(M) \equiv \int_M^{M_8} \dot{M} n(\dot{M}) d\dot{M}.$$

For the SMT formalism we get

$$\sigma(M) = \frac{\delta_c}{\sqrt{2} \Phi^{-1} \left[\Phi\left(-\frac{\delta_c}{\sqrt{2}\sigma_8}\right) - \frac{G(M)}{\bar{\rho}A} \right]}}, \quad (11)$$

where we keep the definition of $G(M)$ and

$$\Phi(x) = \operatorname{erf}(x) + \frac{2^{-p}}{\sqrt{\pi}} \Gamma\left(\frac{1}{2} - p\right) P\left(\frac{1}{2} - p, x^2\right), \quad (12)$$

where p is a parameter in the SMT formalism, and $\Gamma(x)$ and $P(a, x)$ are the gamma and incomplete gamma functions.

Finally, for the J01 prescription,

$$\sigma(M) = \exp \left\{ -\Psi^{-1} \left[\Psi(\ln \sigma_8^{-1}) - \frac{G(M)}{A\bar{\rho}} \right] \right\}, \quad (13)$$

where the function $\Psi(S)$ is given by

$$\Psi(S) = \int_0^S e^{-|x+B|^\varepsilon} dx.$$

In every case the values of Ω and the amplitude of density fluctuations measured in a sphere of $8h^{-1}$ Mpc, σ_8 , are assumed to be known.

If we associate clusters of galaxies with dark matter haloes we can obtain $\sigma(M)$ from an observational estimation of the differential mass function of galaxy clusters, using equations (10), (11) or (13), assuming it is well described by the PS, SMT or J01 formalisms. In order to obtain a realistic $\sigma(M)$ we must ensure that the assumed formalism provides an accurate description of the underlying mass function. The most reliable results will be obtained for the formalism that best describes the mass function, a fact that can be tested using numerical simulations.

3.2 Inverting $P(k)$ from $\sigma(M)$

3.2.1 A First try

As a result of the procedures described in the last section we obtain a set of values $\sigma(R_i)$ for $i = 1, \dots, N_R$. For each one of them we have an equation that relates this variance to the power spectrum $\Delta^2(k)$

$$\sigma^2(R_i) = \int_{-\infty}^{\infty} \Delta^2(k) W^2(kR_i) d \ln(k) \quad (14)$$

This is an integral Fredholm equation, with a kernel function given by the Fourier transform of the window function. With this equation, we are able to recover an estimate of $\Delta^2(k)$ in a set of values k_α $\alpha = 1, \dots, N_k$. Following Dodelson & Gaztañaga (1999) we will use Greek index for quantities in k -space and Latin for those in real-space.

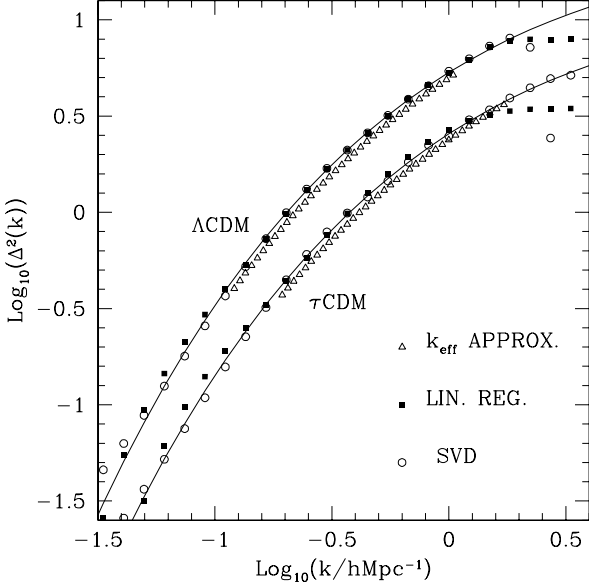


Figure 2. Results of the implementation of the $\Delta^2(k_{eff})$ approximation, SVD and linear regularization to the functions $\sigma(M)$ obtained from the power spectrum of the τ CDM and Λ CDM models

A first and rather simple procedure to achieve this is to use the fact that equation (14) is sharply peaked around a characteristic value of k and only a relatively small interval of k -values contributes to this integral. Then, $\sigma^2(R)$ can then be understood as an average value of the power spectrum in that interval that satisfies the relation (Peacock, 1991; Padilla & Baugh, 2001):

$$\sigma^2(R) = \Delta^2(k_{eff}) \quad (15)$$

for some suitable defined value of k_{eff} .

In fact, if we assume that the power spectrum is a power law $\Delta^2(k) = Ak^n$, this relation is exact and k_{eff} is given by

$$k_{eff} = \frac{1}{R} [9I(n)]^{\frac{1}{n}}, \quad (16)$$

where

$$I(n) = \int_0^\infty y^{n-7} [\sin(y) - y \cos(y)]^2 dy.$$

It is not necessary to assume that the power spectrum behaves like a power law on every scale, as it was mentioned earlier. This can be seen by considering that for a given value of R only a small range in k is important, and locally we can approximate the power spectrum by a power law $\Delta^2(k) \propto k^n$ and so equation (16) is expected to hold at least approximately for this value of n . This is specially true in the case of CDM class power spectra, which benefit from having slowly varying $n(k)$.

We can't use this procedure directly to obtain $\Delta^2(k)$ because equation (16) depends on the index n of the unknown power spectrum. We can avoid this difficulty by either assuming a fixed value for n on every scale (e.g. $n = -2$ for scales corresponding to clusters of galaxies) or by obtaining it from $\sigma(M)$. If $\sigma^2(M)$ behaves like a power law $\sigma^2(R) \propto R^{\tilde{n}}$ and

$$n = -\tilde{n}$$

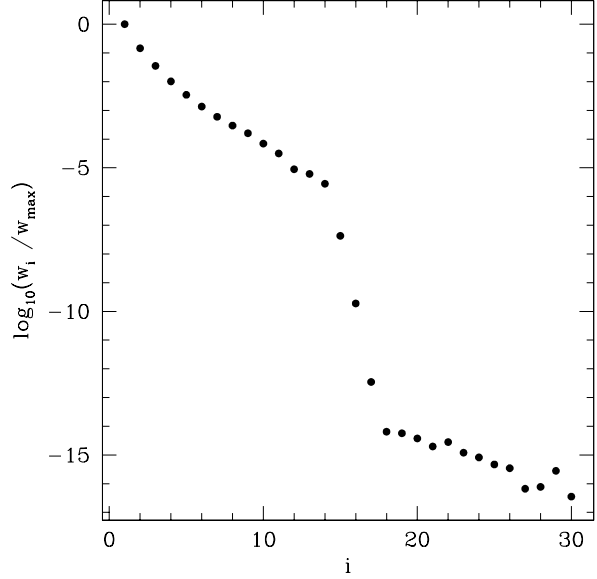


Figure 3. Value of $\log(-\frac{w_i}{w_{max}})$ for the different singular values of the matrix \mathbf{W} . A great quantity of the w_i are very small and are susceptible to roundoff errors.

Figure 2 shows the power spectrum recovered from the function $\sigma(M)$ calculated for a τ CDM and a Λ CDM power spectrum using this method. The range of masses used in this calculation is $10^{12} h^{-1} M_\odot < M < 10^{15} h^{-1} M_\odot$. It is clear from this figure that this procedure gives good results in spite of its simplicity. The solutions obtained for $\Delta^2(k)$ have the correct shape but its amplitude is somewhat underestimated.

3.2.2 Singular Value Decomposition

If we denote by D_α and S_i the values of $\Delta^2(k_\alpha)$ and $\sigma^2(R_i)$, the integral equation (14) can be cast as a matrix, yielding

$$\mathbf{S} = \mathbf{K} \mathbf{D} \quad (17)$$

where \mathbf{K} is the $N_\sigma \times N_k$ kernel matrix and the vectors \mathbf{D} and \mathbf{S} are formed by the values D_α and S_i respectively. Expressed in this way, the first thought about how to obtain a solution is by direct inversion of the kernel matrix, that is

$$\mathbf{D} = \mathbf{K}^{-1} \mathbf{S}. \quad (18)$$

Unfortunately this simple approach does not work. The solutions obtained inverting \mathbf{K} are unstable and often do not have a true physical meaning. This is due to the fact that we try to obtain more information about the power spectrum than is contained in $\sigma(M)$. This situation causes the matrix \mathbf{K} to be numerically singular (although not *strictly* singular).

In order to obtain the best solution \mathbf{D} it is necessary to assume that the errors in S_i obtained from the mass function have a gaussian distribution around their true values \bar{S}_i , then the probability to obtain a vector \mathbf{S} is proportional to $\exp(-\frac{\chi^2}{2})$ where

$$\chi^2 = (\mathbf{S} - \bar{\mathbf{S}})^T C_S^{-1} (\mathbf{S} - \bar{\mathbf{S}}), \quad (19)$$

and C_S is the covariance matrix for \mathbf{S} .

We can relate $\tilde{\mathbf{S}}$ to the true value of the power spectrum by $\tilde{\mathbf{S}} = \mathbf{K}\mathbf{D}$. It is easy to see that the solution \mathbf{D} that minimizes (19) is simply $\mathbf{D} = \mathbf{K}^{-1}\mathbf{S}$, and that its covariance matrix will be given by $C_D = (\mathbf{K}^T C_S^{-1} \mathbf{K})^{-1}$, but, as we mentioned before, this solution does not work. To solve this problem we use the Singular Value Decomposition technique (SVD, see Press et al. 1992). Following Eisenstein & Zaldarriaga (2001), we define $\tilde{K} = C_S^{-\frac{1}{2}} K$ and $\tilde{\mathbf{S}} = C_S^{-\frac{1}{2}} \mathbf{S}$, where $C_S^{-\frac{1}{2}}$ is the inverse matrix of $C_S^{\frac{1}{2}}$ constructed by taking the square root of the eigenvalues of C_S . We then have

$$\chi^2 = |\tilde{K}\mathbf{D} - \tilde{\mathbf{S}}|^2.$$

SVD can be used to find the solution \mathbf{D} that minimizes this quantity. The singular value decomposition of the \tilde{K} matrix is given by $\tilde{K} = U\mathbf{W}V^T$, where U is a $N_R \times N_k$ column orthogonal matrix, \mathbf{W} is an $N_k \times N_k$ diagonal matrix whose entrances w_i are called singular values, and V is an $N_k \times N_k$ orthogonal matrix. With this notation we can express the solution (18) as $\mathbf{D} = \mathbf{V}\mathbf{W}^{-1}\mathbf{U}^T\mathbf{S}$, and the covariance matrix $C_p = \mathbf{V}\mathbf{W}^{-2}\mathbf{V}^T$. If the kernel matrix is singular, then some of the elements w_i of the matrix \mathbf{W} are zero and the inverse matrix \mathbf{W}^{-1} is obviously not defined. But, even when none of the singular values are exactly zero, their values can be so small as to be dominated by the roundoff errors and their inverses w_i^{-1} will have very large values causing the problem to be numerically intractable. Figure 3 shows the singular values w_i obtained by performing the SVD of the matrix K . It can be seen that there are a large number of singular values that are very small causing the problem to be singular.

The solution obtained replacing by zero the quotients w_i^{-1} corresponding to the smallest singular values minimizes equation (19) and is therefore the solution \mathbf{D} that we are looking for (Press et al., 1992).

In Figure 2 is also shown the power spectrum recovered from $\sigma(M)$ by application of the SVD method for the same range of masses than in the $\sigma^2(R) = \Delta^2(k_{eff})$ approximation. It is clear from this figure that SVD gives very good results in a wide range of scales, correctly reproducing the shape and amplitude of the theoretical power spectrum.

3.2.3 Linear Regularization

Another way to obtain a solution for (17) is using a Bayesian approach. As we mentioned before the problem we are trying to solve is singular since we wish to obtain more information about $\Delta^2(k)$ from $\sigma(M)$ than that actually available. To avoid this lack of information we can supply a prior such as the hypothesis of a “smooth” power spectrum. In order to do this we put a second exponential in the probability distribution for \mathbf{S} , which will be proportional to $\exp[-\frac{1}{2}(\chi^2 + \lambda\beta)]$, where

$$\beta = \mathbf{D}^T \mathbf{H} \mathbf{D}. \quad (20)$$

Now we have to find the solution \mathbf{D} that minimizes the weighted sum $\chi^2 + \lambda\beta$. If the minimization of the functional β alone is non-singular, the general minimization will be so too (Press et al., 1992). The first functional (χ^2) is a measure of the concordance of the solution \mathbf{D} with the data \mathbf{S} , the

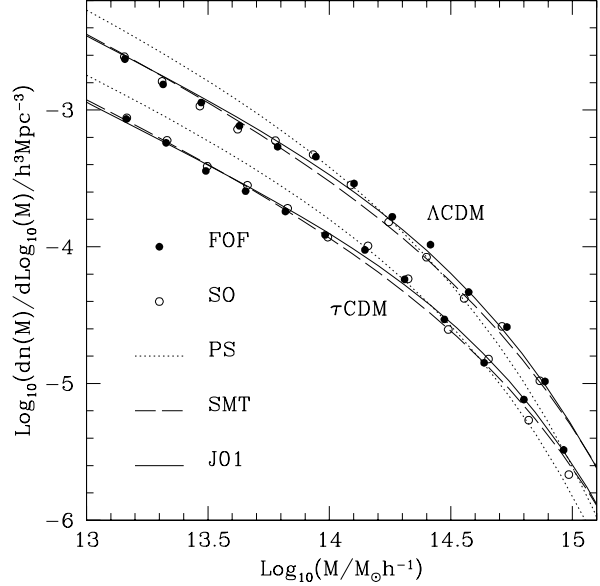


Figure 4. Mass function from the GIF τ CDM and Λ CDM simulations, determined using FOF halo finder compared with the predictions of the PS, SMT and J01 formalisms.

second term (β) can be viewed as a measure of its agreement with a *prior*, implemented by the matrix H , that makes \mathbf{D} not to vary too much. The λ factor in the second term in eq. (20) sets the relative weight of the two functionals. The limit $\lambda \rightarrow 0$ correspond to the minimization of χ^2 . In this work we have chosen the matrix H corresponding to a constant \mathbf{D} (equation 18.5.3 in Press et al., 1992).

With these definitions the solution for \mathbf{D} that minimizes $\chi^2 + \lambda\beta$ can be found by solving the *normal equations*

$$(\tilde{K}^T \tilde{K} + \lambda H) \mathbf{D} = \tilde{K}^T \tilde{\mathbf{S}}$$

and the covariance matrix will be given by

$$C_D = (\tilde{K}^T \tilde{K} + \lambda H)^{-1}.$$

The solutions obtained in this way depend on the value of λ . This must be determined according to our confidence in observational data. A value that gives equal weight to the minimization of the functionals χ^2 and β is given by

$$\lambda = \text{Tr}(\tilde{K}^T \tilde{K}) / \text{Tr}(H). \quad (21)$$

The results of the application of this method can be appreciated in figure 2 where we show the power spectrum recovered from the same $\sigma(M)$ used in K_{eff} and SVD methods. The value of λ adopted is that of (21). It is clear from this figure that Linear Regularization (LR) also provide suitable results for $\Delta^2(k)$ in a wide range of scales.

4 TESTING THE METHOD

4.1 The GIF simulations

To test the capability of the method developed in the last section to recover the true power spectrum from the differential mass function, we applied it to the GIF τ CDM and Λ CDM simulations (Kauffman et al., 1999). The values of

the cosmological parameters for each simulation are listed in Table 1.

In order to apply our method we first determine the mass function of clusters identified in the numerical simulations. We used a Friends Of Friends (FOF) and a Spherical Overdensity (SO) halo finders. The mass function determined in this way is sensitive to the choice of the linking length parameter b and density contrast κ in the FOF and SO algorithm respectively. Both parameters were set in accordance with the spherical collapse model as described in Eke et al. (1996): $b = 0.2$ and $\kappa = 180$ for $\Omega = 1$, and $b = 0.164$ and $\kappa = 324$ for $\Omega = 0.3$.

Table 1: values of the cosmological parameters in the GIF simulations (Kauffman et al., 1999)

Model	Ω_o	Ω_Λ	h	σ_8	Γ	Box
τ CDM	1.0	0.0	0.5	0.6	0.21	$85h^{-1}\text{Mpc}$
Λ CDM	0.3	0.7	0.7	0.9	0.19	$140h^{-1}\text{Mpc}$

The differential mass functions obtained are plotted in Figure 4, where we also plot the predictions from the formalisms of PS, SMT and J01 for comparison. As it can be seen, the results obtained with the two halo finders are in excellent agreement. This allows us to concentrate on only one halo finding algorithm which we choose to be the FOF algorithm. The later choice is based in the fact that this is the algorithm used by J01 in the determination of the values given in §2 for the coefficients in the mass function of equation (9). Another point in support of our choice comes from the argument presented by J01 which states that the universality of the mass function is more evident using FOF than SO. Note that the prediction of the PS formalism fails to reproduce the mass functions obtained from the simulations whereas the SMT and J01 prescriptions give a more accurate result. This is no surprise since the GIF simulations where used to obtain the parameters in the expressions for the mass function in these formalisms.

4.2 The determination of $\sigma(R)$:

The next step in the method described in §3 is the determination of $\sigma(R)$ from $n(M)$ using equations (10) (11) and (13). In doing so, we have only used the mass functions obtained from the simulations for $M > 10^{13}h^{-1}M_\odot$, which is approximately the range that corresponds to clusters of galaxies. Figure 5 shows the results for $\sigma(M)$ obtained in this way for the τ CDM and Λ CDM simulations, together with the $\sigma(M)$ function calculated using (14) and the power spectrum present in each model.

The best solutions for $\sigma(M)$ where obtained by using the J01 formalism, indicating that it gives the best description of the mass function of dark matter halos when these are identified using a FOF algorithm.

The results obtained with the SMT formalism are in good agreement with those obtained using the J01 recipe for the Λ CDM simulation, which is not the case with the τ CDM simulation, showing that this formalism does not describe the τ CDM mass function at the level of accuracy required in our method. The results obtained with the PS formalism differ notably from those obtained from the theoretical model present in the simulations, showing that this repre-

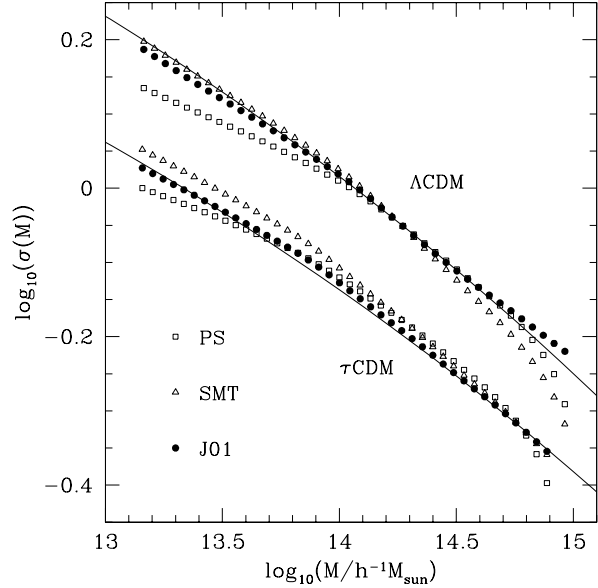


Figure 5. Solutions for $\sigma(M)$ obtained by the application of the different formalisms to the mass functions of the GIF simulations. For clarity the solutions obtained for the τ CDM simulations are divided by a factor 1.25.

sents a poor description of the mass function, a recurrent result in the literature on the subject.

We attempted to determine the covariance matrix C_S for $\sigma^2(M)$ using a bootstrap resampling technique. We determined $n(M)$ for a large number of samples of groups randomly selected from the original list from the simulations. For each of them we calculate $\sigma^2(M)$ according to the PS, SMT and J01 recipes. Following the notation used in §3.2 we estimate the covariance matrix by

$$(C_S)_{ij} = \langle (S_i - \bar{S}_i)(S_j - \bar{S}_j) \rangle$$

where \bar{S} represents the theoretical value of σ^2 for the model considered.

Figure 6 shows the correlation matrix $Cor_{ij} = (C_S)_{ij} / \sqrt{(C_S)_{ii}(C_S)_{jj}}$ obtained with this procedure for the J01 solutions determined from the Λ CDM simulation, the results from using the other formalisms are similar. Note that all masses smaller (bigger) than M_s are correlated. As the mass M only appears in the expressions for $\sigma(M)$ through the function $G(M) = \int_M^{M_s} Mn(M)dM$, the value of $\sigma(M)$ for masses lesser (bigger) than M_s , have no influence on the value of $\sigma(M)$ for masses bigger (lesser) than this limit, so the correlations between these two regions should vanish. This characteristic is not present in the correlation matrix determined by the bootstrap resampling technique, which shows spurious correlations that prove the inadequacy of this technique for the determination of the covariance matrix. We have not succeeded in determining C_S so we assume here a diagonal form. As pointed out by Eisenstein & Zaldarriaga (2001) this simplification may cause an underestimation of the errors in the final power spectrum. For the purpose of this work this is a reasonable approximation, but it has to be properly taken into account if it is aimed to obtain precise constraints upon cosmological models using observational data.

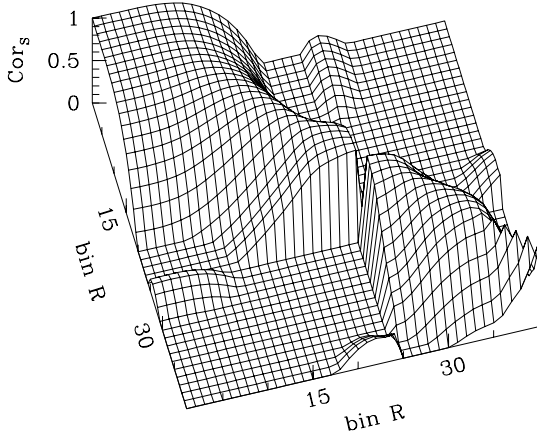


Figure 6. Correlation matrix of the $\sigma^2(M)$ function obtained from the Λ CDM mass function using the J01 formalism. This matrix was calculated using a bootstrap resampling method.

4.3 The determination of $\Delta^2(k)$

Given that in both cases (τ CDM and Λ CDM) the solution $\sigma(M)$ determined using equation (13) with the general fit from J01, is the one that shows a better agreement with that of the corresponding cosmological model, we use this solution to determine the power spectrum assuming that C_S is diagonal. Figure 7 shows the results obtained in this way for the τ CDM and Λ CDM simulations using the different techniques described in §3.2. For comparison we also plot the theoretical power spectrum $\Delta^2(k)$ for each model.

In the implementation of the approximation $\sigma^2(R) = \Delta^2(k_{eff})$ the value of the index n was not determined from $\sigma(R)$ as described in §3.3.1. The solution obtained applying this procedure showed an oscillatory behaviour. Instead, we fixed $n = -2$, and on those scales where this approximation is valid, the obtained power spectrum shows a good agreement with that corresponding to the different models. The solution starts to fail where this approximation ceases to be valid. The solutions recovered have approximately the correct shape, but suffer from the same problem mentioned in §3.2.1, underestimating the amplitude of the power spectrum. This analysis shows that this technique could represent a powerful tool to determine the power spectrum if the index n is determined in a more efficient way.

The solution obtained applying SVD as described in §3.3.2 shows a very good agreement with the correct power spectrum over a wider range of scales in the τ CDM simulation but fails to reproduce the correct shape for the Λ CDM case. This behavior was not present in the solution plotted in figure 2, where the best results were found using this technique. This shows that the solutions obtained using SVD are very sensitive to the differences between the used and exact $\sigma(M)$, and therefore, to the deviations of $n(M)$ with respect to the predictions of the J01 general fit. This indicates that the implementation of the SVD method to real data is not

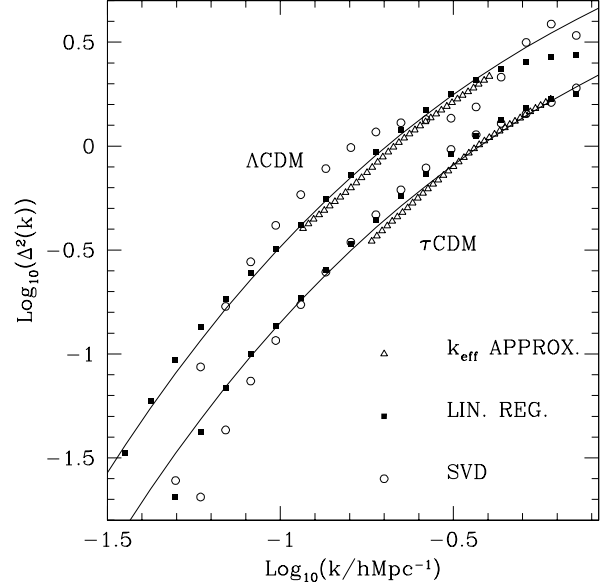


Figure 7. Solutions for $\Delta^2(k)$ obtained with the different techniques of §3.2, using the solution for $\sigma(M)$ determined by de J01 general fit compared with the correct power spectrum of the τ CDM and Λ CDM models.

very efficient, a situation that may improve with the use of the full covariance matrix, instead of a diagonal C_S .

The best solutions were obtained using the LR technique, which reproduces the correct shape and amplitude of the power spectrum over a wide range of scales, showing the same performance that in §3.2.3. This proves that, at least within the hypothesis of a diagonal covariance matrix, this is the best technique to recover the power spectrum from the mass function of galaxy clusters.

It should be stressed the fact that the simulations used in this test are small in volume. Therefore we have not been able to analyze the capacity of our method to deal with the presence of rare massive objects. The formalisms of PS, SMT and J01 have been extensively tested against the results of numerical simulations using volumes much larger than the ones used in this work. These analyses have shown that the SMT and J01 mass functions account properly for the most massive objects. This indicates that the effect of the presence of massive clusters in the mass function will be in perfect agreement with the theoretical formalisms. Further more, the inclusion of these objects in our analysis will improve our results and increase the range of scales in which $\Delta^2(k)$ is recovered, since the numerical problem becomes more easily tractable when a wider range of masses is taken into account.

To test our method in a more realistic situation, we also analyzed the effect of introducing errors in the determinations of individual cluster masses. We constructed 5 samples of groups from the original one identified in the Λ CDM GIF simulation, by adding gaussian errors to the individual masses of amplitudes 10%, 20%, 30%, 40% and 50%. For each of these new samples we determined the mass function. The results obtained show that even an error as large as 50% in the individual mass determinations produces a small overall effect in the low mass end, causing deviations of less than 10% in all cases. In the high mass end

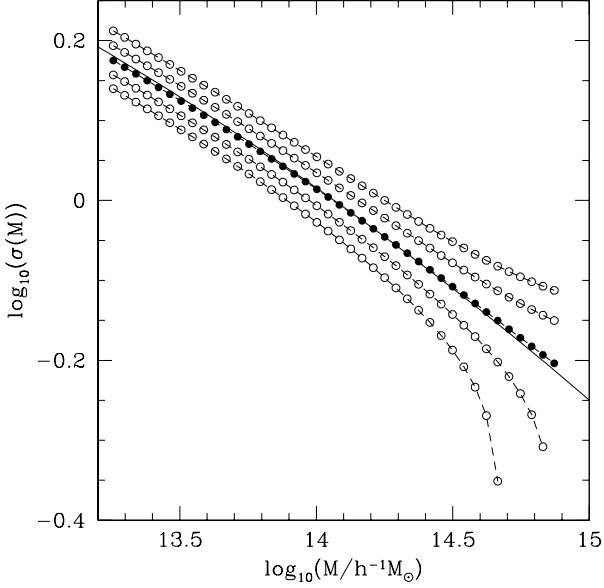


Figure 8. Solutions for $\sigma(M)$ obtained from the mass function of the Λ CDM GIF simulation by the general fit of J01 fixing the values of $\Omega = 0.3$, and varying σ_8 in the values 0.8, 0.85, 0.9, 0.95 and 1.0. Filled circles indicate the solution for $\sigma_8 = 0.9$.

($\log_{10}(M/h^{-1}M_{\odot}) > 14.5$) these errors can produce deviations of even 30% due to the small number of objects. Nevertheless, their presence does not produce a considerable effect in the final power spectrum, indicating that our method is robust even when dealing with large errors in the mass estimates.

4.4 Dependence on Ω and σ_8

The method for the determination of the power spectrum described in §3 requires the prior knowledge of the density parameter Ω and the rms mass fluctuations on some reference scale, for example $R = 8h^{-1}\text{Mpc}$ (σ_8). In this section we analyze the dependence of our results on these parameters. In order to do so we calculate the solution $\sigma(M)$ from the mass function of the Λ CDM simulation ($\Omega = 0.3$, $\sigma_8 = 0.9$) fixing $\Omega = 0.3$ and setting $\sigma_8 = 0.8, 0.85, 0.9, 0.95$, and 1.0, and fixing $\sigma_8 = 0.9$, and varying Ω from 0.2, 0.25, 0.3, 0.35 and 0.4. The results obtained in this way are plotted in Figures 8 and 9.

Figure 8 shows that except for the high mass end, the effect of changing σ_8 in the solutions of $\sigma(M)$ is simply a change in the overall normalization. On the other hand, the shape of the solutions is affected in the high mass limit. As is shown below, this effect propagates into the power spectrum causing differences in the low k end.

Figure 9 shows that the effect of changing the value of Ω can be more serious, as the solutions obtained have different behaviors than that observed in the $\Omega = 0.3$ case. This will cause differences in the obtained power spectrum in all scales.

In order to analyze the effect of these variations on the power spectrum we use the LR technique to obtain $\Delta^2(k)$ from the $\sigma(M)$ functions plotted in Figures 8 and 9. In doing so we used the same value of λ used in §4.3 when obtain-

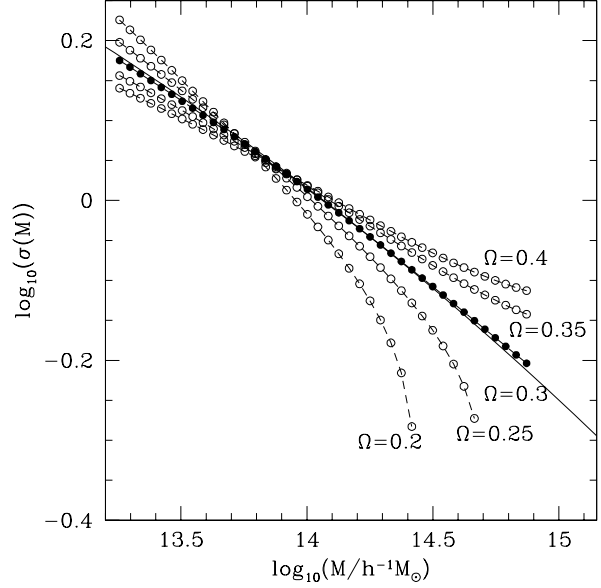


Figure 9. Solutions for $\sigma(M)$ obtained from the mass function of the Λ CDM GIF simulation using the general fit of J01 fixing the values of $\sigma_8 = 0.9$, and varying Ω in the values 0.2, 0.25, 0.3, 0.35 and 0.4. Filled circles indicate the solution for $\Omega = 0.3$.

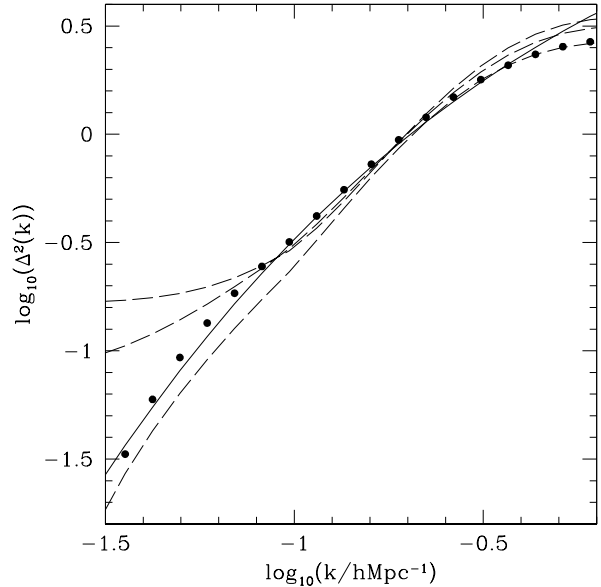


Figure 10. Solutions for $\Delta^2(k)$ obtained applying the LR technique to the solutions for $\sigma(R)$ from the Λ CDM simulation by fixing Ω and varying σ_8 (see Figure 8).

ing the power spectrum from this simulation. The results obtained this way are plotted in Figures 10 and 11.

Figure 10 shows that, as we pointed out previously, the effect arising from changing the value of σ_8 is important in the lower values of k , where it can produce considerable changes in the solutions. For the higher values of k , the solutions obtained are not very different for the one obtained for the correct value of σ_8 . This is the same effect observed in

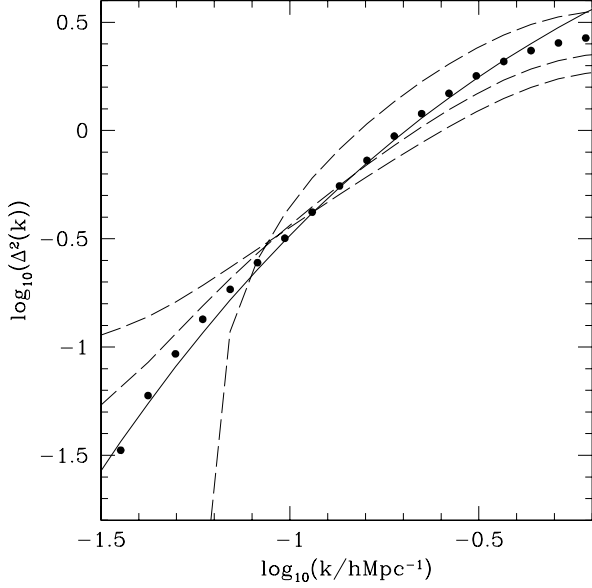


Figure 11. Solutions for $\Delta^2(k)$ obtained applying the LR technique to the solutions for $\sigma(R)$ from the Λ CDM simulation by fixing σ_8 and varying Ω (see Figure 9).

the analysis of $\sigma(M)$ where we only found a renormalization and not a change in shape.

The most important effect on the power spectrum, is that caused by the use of a wrong value of Ω . As it can be seen in Figure 11, the solutions obtained differ notably between them, and show different behavior in every scale. The reason for this is that the effect of changing Ω in $\sigma(M)$ is not a simple renormalization, but a change in the slope of the solutions. This makes Ω the most important parameter in the model.

5 COMPARISON TO THE FKP METHOD

As a final test of our method we compare the outcomes of the method presented in this work, and that of FKP, as described in Zandivarez, Abadi & Lambas (2001).

We applied both methods to the GIF simulations and the results are plotted in Figures 12 and 13 corresponding to the Λ CDM and τ CDM models respectively, where we plot the power spectrum $P(k)$, output of the FKP technique, in logarithmic (upper panel) and linear scales (lower panel). In order to compare these results we have arbitrarily normalized the power spectrum derived from the FKP technique to that of the linear mass power spectrum, which is the outcome of our method.

By inspection to these figures, it is clear that FKP and our method yield similar results, showing the power and performance of our approach. We notice that the solutions for $P(k)$ obtained from the mass function show a much better agreement with the power spectrum of the corresponding model than those obtained using the FKP technique. The range of validity of our solutions must be kept in mind, since the apparent good description of $P(k)$ in the higher values of k correspond to the region where LR gives a constant solution for $\Delta^2(k)$, which in turn gives $P(k)\propto k^{-3}$, the ap-

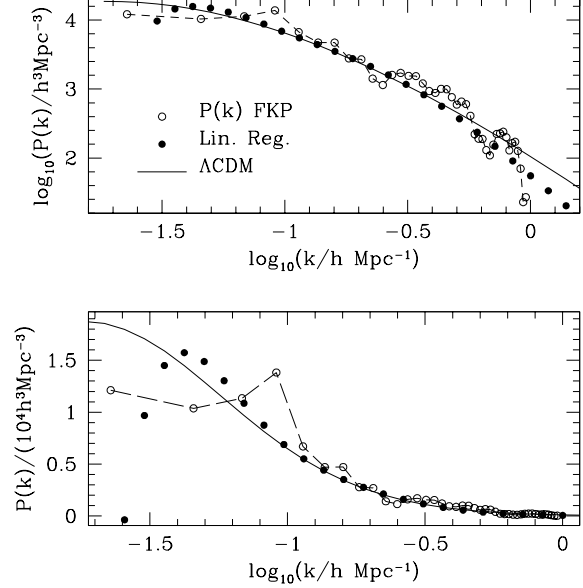


Figure 12. Results obtained for the power spectrum $P(k)$ of the Λ CDM GIF simulation using the LR technique and the FKP method to the same group sample, with logarithmic (upper panel), and linear (lower panel) scales.

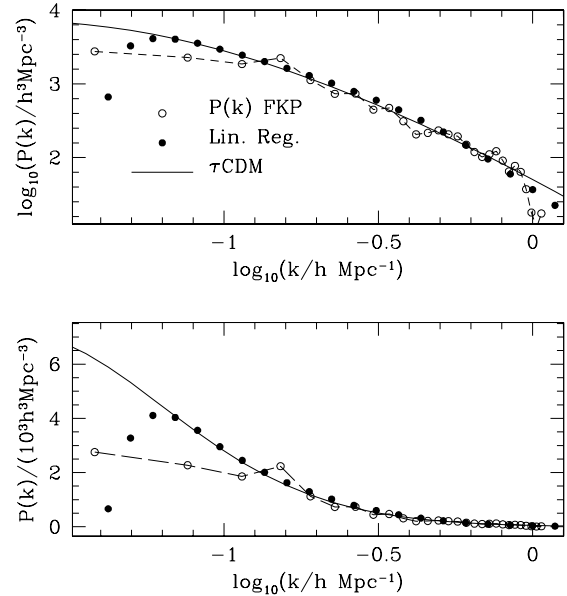


Figure 13. The same as Figure 12, but for the τ CDM GIF simulation.

proximate behavior of the power spectrum in these scales. Even though LR gives a more accurate description of $P(k)$ in the range where it has been proven to be applicable, the estimated power spectrum using the FKP technique works for higher values of k . As the range of validity of our solution depends on the mass range of the differential mass function, the inclusion of low clusters masses will improve this situation.

As it can be seen in the lower panels of Figures 12 and 13, the solution obtained by the use of LR gives a very accu-

rate description of the power spectrum for the lower values of k , where the FKP method fails to give a satisfactory answer. Besides, the logarithmic bins in LR solution's sample these values of k in a better way than the linear bins of the FKP technique, showing that our method is better in studying the power spectrum at these scales.

It is important to stress the fact that our method provides the linear power spectrum, while the solution of the FKP technique is affected by nonlinear effects. These are not important in the range of scales analyzed here, but this may be significant when objects of lower masses are included in the analysis.

A significant and important difference in our technique is that it naturally allows the use of information from different scales and objects, ranging from poor to rich clusters of galaxies in an homogeneous way. On the other hand the FKP technique will give different results for subsets of systems of galaxies with different masses, reflecting their relative bias with respect to the underlying mass distribution. Furthermore, in our method it is desirable the inclusion of objects with a very broad range of masses, since this allows for a better determination of the power spectrum over a wider range of scales.

6 CONCLUSIONS

In this work we have developed a new method to determine the linear mass power spectrum from the mass function of galaxy clusters based on the PS, SMT and J01 formalisms. The rms fluctuation of mass $\sigma(M)$ is determined using the expression for the mass function in the form of a differential equation. We then use different techniques from integral equations theory to obtain the dimensionless power spectrum $\Delta^2(k)$ from $\sigma(M)$.

The implementation of this method to the GIF τ CDM and Λ CDM simulations shows a high efficiency in recovering the correct shape and amplitude of the power spectrum in a wide range of scales, showing a high performance and real practical utility. Although the different solutions for $\sigma(M)$, obtained from the simulations, show an overall agreement, it is clear that the J01 prescription gives a much better result than the PS or SMT formalism, showing that the J01 general fit gives an excellent description of the differential mass function of clusters identified in the simulations.

In the theoretical case analyzed in §3.2 the best solution was that obtained from the implementation of SVD, which recovers the power spectrum in a wide range of scales. However, from the analysis of the results obtained from the simulations we conclude that the best technique to invert the integral equation in our problem is linear regularization. This situation can change with the use of the full covariance matrix and so, it must be analyzed without the assumption of a diagonal C_S .

The comparison of the results obtained with our method with those obtained by the standard FKP technique, shows a very good general agreement. Nevertheless, in the scales of validity of our solutions, our answer gives a much more accurate description of the power spectrum than the ones obtained by the use of the FKP method. This is specially valid in the lower values of k where the FKP solution fails to give the correct answer. Further more, the logarithmic

bins of our method sample these scales in a more efficient way than linear bins (as is the case in the FKP output). This produces important effects in the analysis of the power spectrum in large scales. The FKP technique works for higher values of k than the LR solution. However, this can improve significantly if information of $n(M)$ for lower masses is included in the analysis.

In order to apply our procedure to real data we need an estimate of the mass function of galaxy clusters. Unfortunately, present estimates of this important statistical measure are not completely satisfactory since quoted values are significantly different and moreover they are referred to different cluster mass definitions (see for instance Bahcall & Cen, 1993; Biviano et al., 1993; Girardi et al., 1998; Girardi & Giuricin, 2000; Reiprich & Böhringer, 2001; Bahcall et al., 2002).

As we have already pointed out, even in the case where errors in the individual masses are large, the overall effect in the mass function is not important when compared to other sources of uncertainties such as the use of different mass definitions. Different methods for cluster mass estimates (i.e. optical, x-ray, gravitational lensing) are clearly correlated, but provide different values for the mass of the same cluster. Furthermore, it is not clear how these mass definitions are related to the ones used in numerical simulations (i.e. FOF $b = 0.2$, FOF $b = 0.17$, SO $\kappa = 200$, etc.) which also show differences among them (see White, 2001). This is of extreme importance and is the principal source of uncertainties in our method. Given that observational cluster masses are estimated using one of the methods mentioned above, it may be incorrect to assume a fit to the mass function whose coefficients have been determined using FOF masses, such as the J01 formalism.

This indicates that the use of expressions derived from theoretical formalisms in the analysis of observational data (a common practice in the literature) must not be made without a careful analysis of the relationship between the different mass definitions involved.

There are other statistics available in the literature, such as the temperature function (Henry & Arnaud, 1991; Markevitch, 1998; Blanchard et al., 2000; Ikebe et al., 2001) of X-ray samples. The high correlation between temperature and mass suggested by numerical simulations (Evrard, 1990; Evrard, Metzler & Navarro, 1996; Yoshikawa & Suto, 2000; Mathiesen & Evrard, 2001), has lead many authors to use temperature functions in confronting observations with theoretical predictions, instead of mass functions.

The method described here can equally be applied to the temperature function of galaxy clusters, but, in doing so, we need a reliable mass-temperature relation. Unfortunately this transformation has not been yet determined in an accurate way, and different $T - M$ relations give equally different results between them.

The observational determination of the mass function of galaxy clusters can improve in the next few years with the outcome of new mass estimates from gravitational lenses, or even from virial mass estimates obtained from the new large catalogs that will be soon available such as 2dF and SDSS.

If the above discussion is properly addressed the methods described in this work can be very useful tools to provide new and reliable determinations of the linear mass power spectrum.

ACKNOWLEDGMENTS

We would like to thank Carlthorn Baugh for reading the manuscript and his helpful comments and Ariel Zandivarez for providing us the calculations of the FKP power spectrum. We also want to thank the referee Fabio Governato for his constructive suggestions. AGS also thanks Mario Abadi for his kind help. This work was partially supported by the Concejo Nacional de Investigaciones Científicas y Tecnológicas (CONICET), the Secretaría de Ciencia y Técnica (UNC) and the Agencia Córdoba Ciencia.

REFERENCES

- Bahcall, N. A., Cen, R., 1993, *Apj*, vol 407, L49
- Bahcall, N. A., Dong, F., Bode, P., Kim, R., Annis, J., McKay, T., Hansen, S., Gunn, J., Ostriker, J.P., Postman, M., Nichol, R.C., Tomotsugu, G., Brinkmann, J., Knapp, G.R., Lamb, D.O., Schneider, D.P., Vogeley, M.S., York, D.G., 2002, preprint (astro-ph/0205490)
- Blanchard, A., Sadat, R., Bartlett, J.G., Le Dour, M., 2000, *A&A*, 362, 809B
- Biviano, A., Girardi, M., Giuricin, G., Mardirossian, F., Mezzetti, M., 1993, *ApJ*, 411L, 13
- Bond, J. R., Cole, S., Efstathiou, G., Kaiser, N., 1991, *Apj*, 379, 440
- Colberg, R. G., Couchman, H. M. P., 1989, *Apj*, 340, 47
- Dodelson, S., Gaztañaga, E., 2000, *MNRAS*, 312, 774
- Efstathiou, G., Frenk, C. S., White, S. D. M., Davis, M. 1988, *MNRAS*, 235, 715
- Eisenstein, D. J., Zaldarriaga, M., 2001, *Apj*, 546, 2
- Eke, V. R., Cole, S., Frenk, C. S., 1996, *MNRAS*, 282, 263
- Evrard, A. E., 1990, *Apj*, 363, 349
- Evrard, A. E., Metzler, C.A., Navarro, J. F., 1996, *Apj*, 469, 494
- Feldman, H.A., Kaiser, N., Peacock, J.A., 1994, *Apj*, 426, 23 (FKP)
- Gaztañaga, E., Baugh, C.M., 1998, *MNRAS*, 294, 229
- Girardi, M., Borgani, S., Giuricin, G., Mardirossian, F., Mezzetti, M., 1998, *ApJ*, 506, 45
- Girardi, M., Giuricin, G., 2000, *Apj*, 540, 45
- Governato, F., Babul, A., Quinn, T., Tozzi, P., Baugh, C.M., Katz, N., Lake, G., 1999, *MNRAS*, 307, 949
- Henry, J.P., Arnaud, K.A., 1991, *Apj*, 372, 410
- Ikebe, Y., Reiprich, T.H., Böhringer, H., Tanaka, Y., Kitayama, T., *A&A*, 383, 773
- Jenkins, A., Frenk, C. S., White, S. D. M., Colberg, J. M., Cole, S., Evrard, A. E., Couchman, H. M. P., Yoshida, N., 2001, *MNRAS*, 321, 372 (J01)
- Kauffman, G., Colberg, J. M., Diaferio, A., White, S. D. M., 1999, *MNRAS*, 303, 188
- Markevitch, M., 1998, *Apj*, 504, 27
- Mathiesen, B., Evrard, A. G., 2001, *Apj*, 546, 100
- Padilla, N. D., Baugh, C. M., 2001, preprint (astro-ph/0104313)
- Peacock J. A., Heavens, A., 1989, *MNRAS*, 243, 133
- Peacock J.A., 1991, *MNRAS*, 253, 1
- Press, W. H., Schechter, P., 1974, *Apj*, 187, 425 (PS)
- Press, W. H., Teukosky, S. A., Vetterling, W. T., Flannery B. P., 1992, *Numerical Recipes*, sec. ed., Cambridge University Press
- Reiprich, T.H., Böhringer, H., 2002, *ApJ*, 567, 716
- Sheth, R. K., Tormen, G., 1999, *MNRAS*, 308, 119
- Sheth, R. K., Mo, H. J., Tormen, G., 2001, *MNRAS*, 323, 1 (SMT)
- Tormen, G., 1998, *MNRAS*, 297, 648
- White, M., 2001, *A&A*, 367, 27
- Yoshikawa, K., Jing, Y. P., Suto, Y., 2000, *Apj*, 535, 593
- Zandivarez, A. A., Abadi, M. G., Lambas, D. G., 2001, *MNRAS*, 326, 147

APPENDIX A: OBTAINING $\sigma(M)$ FROM THE PS, SMT AND J01 FORMALISMS

The expression for the mass function in the PS, SMT and J01 formalisms can be re-interpreted as differential equations to obtain $\sigma(M)$ from $n(M)$. If we use the PS formalism then the mass function is given by:

$$n(M, z)dM = \sqrt{\frac{2}{\pi}} \frac{\bar{\rho}}{M^2} \frac{\delta_c}{\sigma(M, z)} \left| \frac{d \ln(\sigma)}{d \ln(M)} \right| e^{-\left(\frac{\delta_c^2}{2\sigma^2(M, z)}\right)} dM$$

that can be written as

$$Mn(M)dM = -\sqrt{\frac{2}{\pi}} \frac{\bar{\rho}}{\sigma^2} e^{-\left(\frac{\delta_c^2}{2\sigma^2}\right)} \frac{d\sigma}{dM} dM$$

where all dependence on σ is in the right hand side. Integrating in both sides with respect to M between a mass M and $M_8 = \frac{4\pi}{3} \bar{\rho} (8h^{-1} Mpc)^3$ corresponding to a sphere of uniform density and radius $R = 8h^{-1} Mpc$, we get

$$G(M) \equiv \int_M^{M_8} \dot{M} n(\dot{M}) d\dot{M} = \bar{\rho} \frac{2}{\sqrt{\pi}} \left[\int_{\mu_M}^{\mu_8} e^{-\mu^2} d\mu \right] \quad (A1)$$

where $\mu = \frac{\delta_c}{\sqrt{2}\sigma(M)}$ and $\mu_8 = \frac{\delta_c}{\sqrt{2}\sigma_8}$.

Using the definition of the error function

$$\text{erf}(x) = \frac{2}{\sqrt{\pi}} \int_0^x e^{-\mu^2} d\mu$$

and using the value of σ_8 as a constant of integration, (A1) can be expressed as

$$G(M) = \bar{\rho} \left[\text{erf}\left(\frac{\delta_c}{\sqrt{2}\sigma_8}\right) - \text{erf}\left(\frac{\delta_c}{\sqrt{2}\sigma(M)}\right) \right]$$

and then we obtain the expression for $\sigma(M)$ given in equation (10)

$$\sigma(M) = \frac{\delta_c}{\sqrt{2} \text{erf}^{-1} \left[\text{erf}\left(\frac{\delta_c}{\sqrt{2}\sigma_8}\right) - \frac{G(M)}{\bar{\rho}} \right]}$$

If we assume the validity of the SMT formalism then the differential equation for $\sigma(M)$ is

$$Mn(M)dM = -\sqrt{\frac{2}{\pi}} A \bar{\rho} \frac{\sqrt{a} \delta_c}{\sigma^2} \left[1 + \left(\frac{\sigma}{\sqrt{a} \delta_c} \right)^{2p} \right] e^{-\left(\frac{a \delta_c^2}{2\sigma^2}\right)} \frac{d\sigma}{dM} dM$$

This is a little more complicated than the corresponding to the PS formalism but can be solved in an analogous way. Integrating between M and M_8 we get

$$G(M) = A \bar{\rho} \frac{2}{\sqrt{\pi}} \left[\int_{\mu_M}^{\mu_8} e^{-\mu^2} d\mu + 2^{-p} \int_{\mu_M}^{\mu_8} \mu^{-2p} e^{-\mu^2} d\mu \right] \quad (A2)$$

where $G(M)$ is given by (A1) and now $\mu = \sqrt{\frac{a}{2}} \frac{\delta_c}{\sigma(M)}$.

The first term of the right hand side in (A2) is the same than in the PS formalism and is equal to $\text{erf}(\mu) |_{\mu_M}^{\mu_8}$, the difference in this case is given by the second term. If we use the definition of the *incomplete gamma function*

$$P(a, x) = \frac{1}{\Gamma(a)} \int_0^x t^{a-1} e^{-t} dt \quad a > 0$$

we can see easily that

$$\begin{aligned} \int_0^{\mu_M} \mu^{-2p} e^{-\mu^2} d\mu &= \frac{1}{2} \int_0^{\mu_M^2} t^{-(p+\frac{1}{2})} e^{-t} dt \\ &= \frac{1}{2} \Gamma\left(\frac{1}{2} - p\right) P\left(\frac{1}{2} - p, \mu_M^2\right) \end{aligned}$$

Then, if we define the function

$$\Phi(x) = \text{erf}(x) + \frac{2^{-p}}{\sqrt{\pi}} \Gamma\left(\frac{1}{2} - p\right) P\left(\frac{1}{2} - p, x^2\right)$$

we can write (A2) as

$$G(M) = A\bar{\rho} \left[\Phi\left(\frac{\delta_c}{\sqrt{2}\sigma_8}\right) - \Phi\left(\frac{\delta_c}{\sqrt{2}\sigma(M)}\right) \right]$$

from where we obtain the expression for $\sigma(M)$ in the SMT formalism given in equation (11)

$$\sigma(M) = \frac{\delta_c}{\sqrt{2}\Phi^{-1}\left[\Phi\left(\frac{\delta_c}{\sqrt{2}\sigma_8}\right) - \frac{G(M)}{A\bar{\rho}}\right]}$$

It is possible to consider that the J01 mass function gives a more accurate description of the real behavior of the mass function. If this is the case, then we use the expression

$$n(M, z)dM = \frac{A\bar{\rho}(z)}{M^2} \frac{d\ln(\sigma^{-1})}{d\ln(M)} e^{-(|\ln(\sigma^{-1}+B)|^\epsilon)} dM$$

which must be re-interpreted as a differential equation for $\sigma(M)$ as a function of $n(M, z)$. This expression can be written as

$$Mn(M)dM = A\bar{\rho}e^{-(|S+B|^\epsilon)} \frac{dS}{dM} dM$$

where $S \equiv \ln(\sigma^{-1}) = -\ln(\sigma)$. Integrating in both sides with respect to M between M and M_8 and keeping the definition of $G(M)$, we get

$$G(M) = A\bar{\rho}(\Psi(S_8) - \Psi(S))$$

where

$$\Psi(S) = \int_0^S e^{-|x+B|^\epsilon} dx$$

Then we can write

$$S = \Psi^{-1}\left[\Psi(S_8) - \frac{G(M)}{A\bar{\rho}}\right]$$

from where we get the following expression for $\sigma(M)$

$$\sigma(M) = \exp\left\{-\Psi^{-1}\left[\Psi(\ln \sigma_8^{-1}) - \frac{G(M)}{A\bar{\rho}}\right]\right\}$$

which is given in equation (13).